*Life-Cycle of Structures and Infrastructure Systems – Biondini & Frangopol (Eds)*
*© 2023 The Author(s), ISBN 978-1-003-32302-0*
*Open Access: www.taylorfrancis.com, CC BY-NC-ND 4.0 license*

# Stochastic load-carrying capacity assessment of brick masonry arch bridges

B. Liu
*School of Civil Engineering, University of Leeds, Leeds, UK*

I.B. Muhit
*School of Civil Engineering, University of Leeds, Leeds, UK*
*School of Computing, Engineering & Digital Technologies, Teesside University, Middlesbrough, UK*

V. Sarhosis
*School of Civil Engineering, University of Leeds, Leeds, UK*

ABSTRACT: Masonry arch bridges form an integral part of our infrastructure network, and their safety is important for the functioning of our society. Now, assessing the structural performance of ageing masonry infrastructure is a complex task. Existing ageing masonry arch bridges are characterized by inherent variability and may have stochastic material properties even in the same bridge. Hence, a realistic methodology for structural assessment of masonry arch bridges is crucial to protect the ageing masonry bridges and utilize these resources efficiently. In this study, stochastic-based assessment on the load-carrying capacity of masonry arch bridges has been performed, which introduces material variabilities into a two-dimensional structural analysis model based on the Discrete Element Method (DEM). Over 100 probabilistic analyses have been developed to assess the ultimate load that a bridge can carry when subjected to monotonic loading at a quarter span. The bond properties of mortar joints, including cohesion, tensile strength, and friction angle, were considered as stochastic variables following a normal distribution. The computational results were compared against the experimental results obtained from the literature. From the results analysis, it was shown that the computational model considering the random variability of bond strength properties can better predict the load-carrying capacity of the masonry arch bridge than the deterministic one. The bond strength at the unit-to-mortar interface significantly affected the ultimate strength of the masonry arch bridge.

## 1 INTRODUCTION

Masonry arch bridges form a significant part of the UK and European infrastructure network. It is estimated that there are approximately 200,000 masonry arch bridges and culverts in Europe and 40,000 masonry arch bridges in the UK. Most of these bridges were constructed between the 17th and 19th centuries and are still in service today (Forgács et al. 2021). After being used for over a hundred years, the significant structural deterioration caused by several environmental impacts may result in a reduction in the durability and load-bearing capacity of the bridges. On the other hand, most of these old masonry arch bridges support traffic loads much higher than those originally designed to carry, which can pose a serious threat to the safety of the bridges. Thus, there is an urgent need to assess the in-service behavior and predict the load-bearing capacity of masonry arch bridges to inform their repair, maintenance, and rehabilitation strategies.

Assessing the structural performance of ageing masonry arch bridges is challenging due to the inherent variability in their material properties. So far, several computational approaches, ranging from simple to high-fidelity, have been developed to predict the ultimate load-carrying capacity of

DOI: 10.1201/9781003323020-171

masonry arch bridges (D'Altri et al. 2019). Within these numerical methods, a large number of input parameters are required to describe the mechanical behavior of materials and define the interactions between different elements. These parameters need to be carefully selected so that the model can accurately reproduce the behavior of real structures (Sarhosis & Sheng 2014).

Now, in order to assess the influence of material variability on the ultimate load-carrying capacity of masonry structures, high fidelity numerical modelling approaches coupling with Monte-Carlo simulations have been used (Li et al. 2014, Muhit et al. 2022). For example, Sarhosis et al. (2019) proposed a methodology which considers the spatial variability of masonry materials. The proposed method was integrated into a two-dimensional (2D) discrete element modelling approach to predict the stochastic strength of masonry walls containing openings. The study also carried out a series of sensitivity analyses to determine the factors affecting the load-carrying capacity of masonry walls. Later, the approach was adopted and incorporated within the three-dimensional (3D) Discrete Element Method (DEM) software for assessing the mechanical behavior of other masonry structures (Pulatsu et al. 2022, Gonen et al. 2022).

Following the research carried out by Sarhosis et al. (2019), this paper presents a stochastic-based assessment of the load-carrying capacity of masonry arch bridges subjected to static load. More than 100 realizations were carried out on a masonry arch bridge model developed based on the 2D DEM. Computational results were compared against the experimental findings obtained from the literature. The stochastic parameters considered in the current study included the friction angle, tensile strength, and cohesion at the unit-to-mortar interface, representing the bond properties of mortar joints. Moreover, sensitivity analysis was carried out to investigate the influence of these mortar bond properties on the load-carrying capacity of the masonry arch bridge.

## 2 METHODOLOTY

The heterogeneity and inherent variability in material properties are the most remarkable characteristics of ageing masonry arch bridges, which considerably affect the structural behavior and load-carrying capacity of the bridge. However, most of the computational models in previous research have failed to consider material variabilities. In other words, the same (uniform) material parameters were usually assigned throughout the masonry domain by engineers/researchers (Sarhosis et al. 2019). This study has adopted a probabilistic approach to investigate the influence of random material properties on the mechanical behavior of masonry arch bridges. The framework of the methodology adopted in this study is summarized in Figure 1.

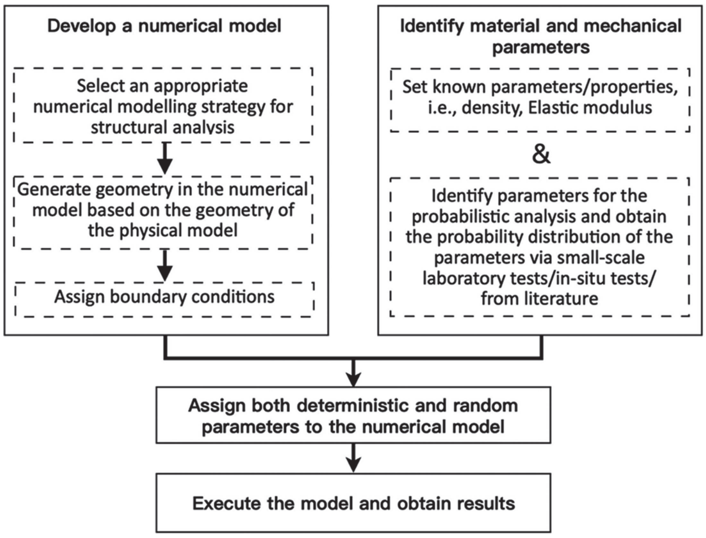

Figure 1. Framework for introducing material variabilities in computational models.

Overall, the methodology involved introducing material variabilities into the computational model. As the first step, the critical parameters for the probabilistic analysis need to be identified, and the mean values and probability distributions of these parameters can be obtained from either small-scale laboratory/in-situ tests or the literature. Having assigned deterministic and stochastic parameters to the computational model, simulations and sensitivity analyses can then be executed. It is worth noting that the parameters used for the probabilistic analysis should be selected based on the characteristics of the structure. For example, as the low bond strength of mortar joints has been found to be one of the dominant factors affecting the mechanical behavior of historical masonry arch bridges (Sarhosis et al. 2019), the bond properties of the unit-to-mortar interface, including friction angle, tensile strength, and cohesion, have been selected as random variables for probabilistic analysis in the study.

## 3 EXPERIMENTAL TESTING OF A MASONRY ARCH WITH BACKFILL

Full-scale static tests on brickwork masonry arch bridges were carried out by Augusthus-Nelson et al. (2018, 2020) at the University of Salford. Figure 2 shows the experimental setup and dimensions for the test chamber and the bridge model. The test was carried out under plain-strain conditions with two stiff walled chambers to restrict any out-of-plane movement of the fill and arch barrel. Class A Engineering bricks and a lime mortar with a mix ratio of 1:2:9 (cement:lime:sand) were used to construct the bridge model to produce the low bond strength characteristic found in real masonry arch bridges.

The experimental model mainly contained an arch barrel constructed with a header bond configuration. The span and thickness of the arch barrel were equal to 3 m and 0.215 m, respectively, and the span-to-rise ratio of the arch was 4:1. The cohesionless MOT type I limestone was selected as the backfill material, which was placed into the test chamber and compacted layer by layer until it reached the 0.3 m over the crown of the arch. During the test, a monotonic load was applied by a hydraulic actuator via a load-spreading beam to the level surface of the backfill above the quarter of the arch barrel.

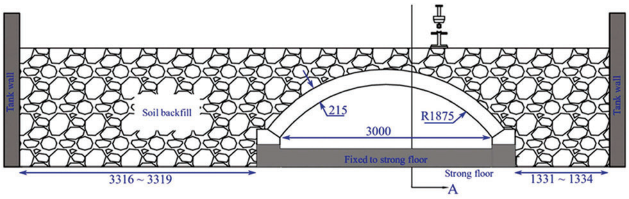

Figure 2. Masonry arch bridge model tested in the laboratory (Augusthus-Nelson et al. 2018).

## 4 DISCRETE ELEMENT MODELLING AND THE COMPUTATIONAL MODEL

Past experience has demonstrated that cracking in masonry arch bridges occurs at the unit-to-mortar interfaces due to the low tensile and shear resistance of the mortar joints. This characteristic makes the discontinuum modelling approach more appropriate compared with other approaches (e.g., homogeneous ones) in simulating the cracking behavior and failure mechanism of masonry arch bridges. In this study, the 2D commercial software, Universal Distinct Element Code (UDEC), based on the DEM, was used to develop the numerical model (Itasca 2011).

Developing a model in UDEC starts with creating a single block covering the domain to be analyzed. Then, the original block generated is discretized into several small blocks in accordance with the geometry feature of the target structures. In the numerical model shown in Figure 3, the arch barrel was assembled by several individual bricks, which were represented by independent deformable blocks with a linear elastic behavior. Mortar joints were represented by zero-thickness interface elements between blocks as shown in Figure 4a. The mechanical behavior of joints in the normal and shear directions (see Figure 4b and c) are subjected to the following equations:

$$\Delta\sigma_n = -K_n \Delta u_n \tag{1}$$

$$\Delta\tau_s = -K_s \Delta u_s \tag{2}$$

where $\Delta\sigma_n$ and $\Delta\tau_s$ are the change in normal and shear stress, respectively; $K_n$ and $K_s$ stand for the stiffness in the normal and shear directions, respectively; and $\Delta u_n$ and $\Delta u_s$ are the change of displacement in the normal and shear directions, respectively.

The numerical model developed in the present work had the same geometry and dimensions as the large-scale bridge tested in the laboratory. Table 1 lists the material and mechanical properties of masonry units, backfill, and backfill-to-arch ring interfaces in the numerical model. These parameters were kept constant (deterministic) throughout the stochastic analysis. On the other hand, material properties of mortar joints, including the tensile strength ($J_{ten}$), cohesion ($J_{coh}$), and friction angle ($J_{fric}$) were considered stochastic to isolate the influence of remaining parameters (i.e., backfill properties and backfill-to-arch ring interface properties) on the load-carrying capacity of the masonry arch bridge and highlight the effect of bond properties with inherent variability found in most real masonry arch bridges. The mean and coefficient of variations (COV) of the stochastic parameters are listed in Table 2 which were obtained from material characterization tests in the laboratory. $J_{coh}$ and $J_{fric}$ were assumed to be normally distributed (Gaussian distribution) while $J_{ten}$ was assumed fully correlated to $J_{coh}$ according to the following equation (Milani & Lourenco 2013):

$$J_{ten} = J_{coh} / 1.4 \tag{3}$$

In terms of loading and boundary conditions of the computational model, the blocks representing the tank walls, basement, and abutments were considered fixed. A monotonic load was applied by controlling a block with the same width as the load-spreading beam to move downwards at a constant velocity. It is worth noting that adaptive damping was assigned to the model to obtain a convergent static solution. In this way, the large displacement of blocks was allowed with the sequential contact detection and update.

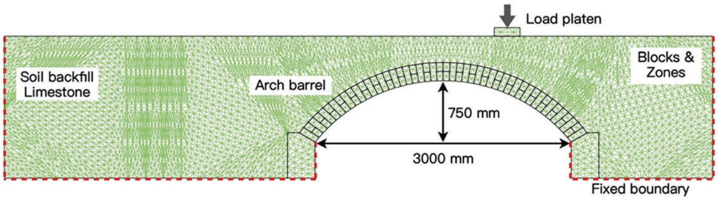

Figure 3. 2D numerical model of the masonry arch bridge based on the DEM showing meshing at the backfill and arch barrel.

## 5 RESULTS AND DISCUSSION

Figure 5a shows a typical failure mechanism of the masonry arch bridge obtained from the computational model. From all simulations, the same four-hinge failure mechanism was observed, with high compressive stresses concentrated at the hinge locations, which was consistent with the experimental observation (see Figure 5b). In particular, with the downward movement of the load platen, a tensile crack initiated at the intrados of the arch underneath the load platen, forming one hinge at the quarter of the arch. The other three hinges occurred

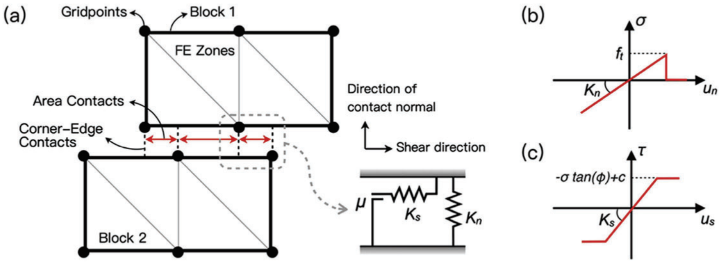

Figure 4. (a) Contacts between blocks; Mechanical behavior of the zero-thickness interface at the (b) normal and (c) shear direction.

Table 1. Material and mechanical properties of masonry units, backfill and backfill-to-arch interfaces adopted in the numerical model (assumed).

| Material | Unit weight | Young's modulus | Poisson's ratio | Friction angle | Tensile strength | Cohesion |
|---|---|---|---|---|---|---|
| Units | $kN/m^3$ | MPa | - | degree | MPa | MPa |
| Backfill | 20 | 300 | 0.3 | 45 | 0 | 0.0005 |
| Bricks | 22 | 9 | 0.2 | - | - | - |
| Backfill-to-arch interface | - | - | - | 35 | 0 | 0 |

Table 2. Statistics of the bond properties of unit-to-mortar interfaces.

| Property | Symbol | Mean value | COV | Distribution |
|---|---|---|---|---|
| Unit-to-mortar interface friction angle | $J_{fric}$ | 35 degrees | 0.06 | Normal |
| Cohesion at the unit-to-mortar interface | $J_{coh}$ | 0.02 MPa | 0.2 | Normal |
| Tensile strength at the unit-to-mortar interface | $J_{ten}$ | $J_{ten} = J_{coh}/1.4$ | - | - |

at approximately the two edges and three-quarters of the arch barrel. Furthermore, the independence of the failure mechanism from the unit-to-mortar bond characteristics suggested that the failure mechanism of the masonry arch bridge was governed by the boundary conditions and bond configurations of the arch barrel, rather than by the material properties of mortar joints.

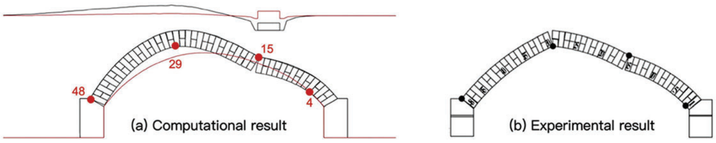

(a) Computational result

(b) Experimental result

Figure 5. Failure mechanism and deformation of the masonry arch bridge obtained from the (a) computational (magnitude factor is 5) and (b) experimental model.

Figure 6 compares the numerical results against the experimental load-displacement relationships of the masonry arch bridge. The mean values for $J_{fric}$ and $J_{coh}$ were equal to 35 degrees and 0.02 MPa, respectively, and the respective COV of these two parameters were equal to 6% and 20%. As the load platen moved downwards, the load carried by the bridge increased until it reached a peak. The fluctuations and reductions observed in the load-displacement curves were related to the crack initiation and propagation process, as well as the stiffness degradation of the bridge under loading. The results also illustrated the influence of the stochastic bond strength properties on the load-carrying capacity of the masonry arch bridge. In principle, a relatively large range of ultimate loads, from 124.33 kN to 273.65 kN, was obtained from the computational model with stochastic bond strength properties. The experimental model had an ultimate load of 142.7 kN, which fell within the range obtained from the computational model and was closer to the lower limit of the range.

Figure 7 shows the sensitivity analysis results of the ultimate load on the bond strength of the mortar joint. In numerical simulations, the mean values of $J_{coh}$ varied from 0.015 MPa to 0.04 MPa with a COV of 20%. The values of tensile strength and cohesion were fully correlated according to Equation 3. For all the simulations, the mean value and COV for $J_{fric}$ remained at 35 degrees and 6%, respectively. In Figure 7, the red lines are trend curves for the maximum, average, and minimum loads obtained from the simulations. It was calculated that the standard deviations for the results of four groups with different mean values of bond strength were all equal to approximately 40%, which highlighted the influence of stochastic bond properties of the unit-to-mortar interface on the ultimate load of the masonry arch bridge. With the stochastic properties of mortar joints, a range of peak loads was obtained from the computational model with different mean values of cohesion and tensile strength. Nevertheless, a significant positive correlation between the bond strength and ultimate loads was observed. With the increase in the mean bond strength, the average load-carrying capacity of the bridge increased, suggesting that the bonding strength of the mortar joints is one of the dominant factors affecting the overall strength of the masonry arch bridge.

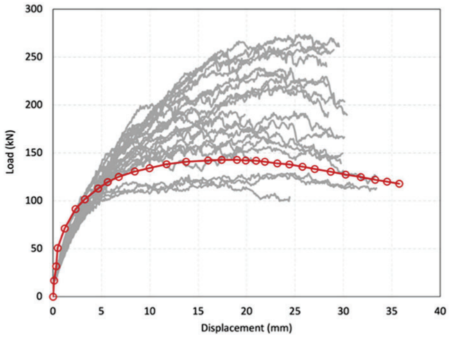

Figure 6. Experimental (red line) against numerical (grey lines) load-displacement curves.

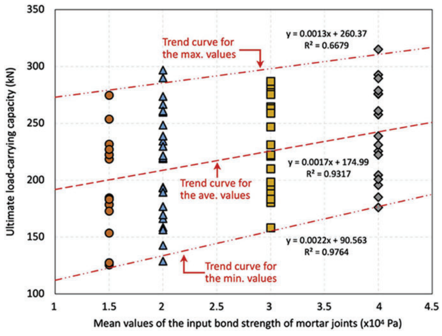

Figure 7. Sensitivity of the ultimate load on the bond strength of mortar joints (the mean value of Jcoh at the unit-to-mortar interface varied from 0.015 MPa to 0.04 MPa, with COV remaining at 20%).

## 6 CONCLUSION

Ageing masonry arch bridges are characterized by inherent variability and may have stochastic material properties even in the same bridge. Such random properties could result in a considerable variation in the strength and stiffness of the masonry arch bridge. However, most of the previous studies have ignored this variation in material properties and instead assigned the same (uniform) parameters through the masonry structure for simplicity, which can lead to an inaccurate evaluation of the ultimate strength of a real masonry arch bridge.

This paper presents a stochastic-based assessment of the ultimate strength and mechanical behavior of masonry arch bridges to address this issue. Stochastic bond properties of unit-to-mortar interfaces were assigned to a 2D computational model developed based on the DEM, and over 100 simulations were executed to predict the load-carrying capacity of the masonry arch bridge. From the analyses of the results, it is shown that the computational model with stochastic material properties can better predict the load-carrying capacity of a real masonry arch bridge with inherent material variabilities. Moreover, the random bond properties did not affect the failure mechanism of the masonry arch bridge investigated and all computational models had a four-hinged behavior. However, with the stochastic bond strength of unit-to-mortar interfaces, the predicted ultimate loads of the bridge had a variation with a COV of approximately 40%, which is expected as the mean value of bond strength increased, the load-carrying capacity of the bridge increased significantly.

The study reported herein is the preliminary findings of the more sophisticated computational model being developed. Hence, such finding assumes and considers the simplest case, while more complicated scenarios like spatially variable bond strength properties of masonry, the correlation between unit-to-mortar interfaces in the same course and different courses, complicated statistical relationships between strength properties, more sophisticated considerations of the backfill materials, etc. can be considered in future studies.

## ACKNOWLEDGEMENT

This work was funded by the EPSRC project “Exploiting the resilience of masonry arch bridge infrastructure: a 3D multi-level modelling framework” (ref. EP/T001348/1). The financial contribution is very much appreciated.

## REFERENCES

Augusthus-Nelson L. & Swift G. 2020. Experimental investigation of the residual behavior of damaged masonry arch structures. *Structures* 27: 2500–12.

Augusthus-Nelson L., Swift G., Melbourne C., Smith C. & Gilbert M. 2018. Large-scale physical modelling of soil-filled masonry arch bridges. *International Journal of Physical Modelling in Geotechnics* 18: 81–94.

D’Altri A.M., Sarhosis V., Milani G., Rots J., Cattari S., Lagomarsino S., Sacco E., Tralli A., Castellazzi G. & de Miranda S. 2019. A review of numerical models for masonry structures. In B. Ghiassi & G. Milani (eds), *Numerical Modeling of Masonry and Historical Structures*: 3–53. Woodhead Publishing.

Forgács T., Sarhosis V. & Ádány S. 2021. Shakedown and dynamic behavior of masonry arch railway bridges. *Engineering Structures* 228: 111474.

Gonen, S., Pulatsu, B., Erdogmus, E., Lourenço, P.B. & Soyoz, S. 2022. Effects of spatial variability and correlation in stochastic discontinuum analysis of unreinforced masonry walls. *Construction and Building Materials* 337: 127511.

ITASCA 2011. *UDEC-universal distinct element code manual: theory and background*. Itasca Consulting Group, Minneapolis.

Li J., Masia, M.J., Stewart, M.G. & Lawrence, S.J. 2014. Spatial variability and stochastic strength prediction of unreinforced masonry walls in vertical bending. *Engineering Structures* 59: 787–797.

Milani, G. & Lourenco, P.B. 2013. Simple Homogenized Model for the Nonlinear Analysis of FRP Strengthened Masonry Structures. II: Structural Applications. *Journal of Engineering Mechanics* 139(1): 77–93.

Muhit, I.B., Masia, M.J., Stewart, M.G. & Isfeld, A.C. 2022. Spatial Variability and Stochastic Finite Element Model of Unreinforced Masonry Veneer Wall System Under Out-of-plane Loading. *Engineering Structures* 267: 114674.

Pulatsu, B., Gonen, S., Parisi, F., Erdogmus, E., Tuncay, K., Funari, M.F. & Lourenço, P.B. 2022. Probabilistic approach to assess URM walls with openings using discrete rigid block analysis (D-RBA). *Journal of Building Engineering* 61: 105269.

Sarhosis V., Forgács T. & Lemos J.V. 2019. Stochastic strength prediction of masonry structure: a methodological approach or a way forward? *RILEM Technical Letters* 4: 122–129.

Sarhosis V. & Sheng Y. 2013. Identification of material parameters for low bond strength masonry. *Engineering Structure* 60:100–10.